THE JOURNAL OF BIOLOGICAL CHEMISTRY VOL. 292, NO. 4, pp. 1510–1523, January 27, 2017

Endoplasmic Reticulum Stress and Ca^{2+} Depletion Differentially Modulate the Sterol Regulatory Protein PCSK9 to Control Lipid Metabolism*

Received for publication, June 17, 2016, and in revised form, November 8, 2016 Published, JBC Papers in Press, December 1, 2016, DOI 10.1074/jbc.M116.744235

Paul Lebeau[‡], Ali Al-Hashimi[‡], Sudesh Sood[‡], Šárka Lhoták[‡], Pei Yu[§¶], Gabriel Gyulay[‡], Guillaume Paré[‖], S. R. Wayne Chen[1], Bernardo Trigatti[§¶], Annik Prat[‡‡], Nabil G. Seidah[‡‡], and Richard C. Austin[‡§2]**

*From the [‡]Department of Medicine, Division of Nephrology, McMaster University and St. Joseph's Hamilton Healthcare and Hamilton Centre for Kidney Research, Hamilton, Ontario L8N 4A6, the [§]Thrombosis and Atherosclerosis Research Institute, Hamilton Health Sciences and McMaster University, Hamilton, Ontario L8L 2X2, the [¶]Department of Biochemistry and Biomedical Sciences, McMaster University, Hamilton, Ontario L8S 4L8, the [‖]Population Health Research Institute and the Departments of Medicine, Epidemiology and Pathology, McMaster University, Hamilton, Ontario L8L 2X2, the **Libin Cardiovascular Institute of Alberta, Department of Physiology and Pharmacology, University of Calgary, Calgary, Alberta T2N 2T9, and the [‡‡]Laboratory of Biochemical Neuroendocrinology, Clinical Research Institute of Montreal, affiliated with the University of Montreal, Montreal, Quebec H2W 1R7, Canada*

Edited by Roger J. Colbran

Accumulating evidence implicates endoplasmic reticulum (ER) stress as a mediator of impaired lipid metabolism, thereby contributing to fatty liver disease and atherosclerosis. Previous studies demonstrated that ER stress can activate the sterol regulatory element-binding protein-2 (SREBP2), an ER-localized transcription factor that directly up-regulates sterol regulatory genes, including *PCSK9*. Given that PCSK9 contributes to atherosclerosis by targeting low density lipoprotein (LDL) receptor (LDLR) degradation, this study investigates a novel mechanism by which ER stress plays a role in lipid metabolism by examining its ability to modulate PCSK9 expression. Herein, we demonstrate the existence of two independent effects of ER stress on PCSK9 expression and secretion. In cultured HuH7 and HepG2 cells, agents or conditions that cause ER Ca^{2+} depletion, including thapsigargin, induced SREBP2-dependent up-regulation of PCSK9 expression. In contrast, a significant reduction in the secreted form of PCSK9 protein was observed in the media from both thapsigargin- and tunicamycin (TM)-treated HuH7 cells, mouse primary hepatocytes, and in the plasma of TM-treated C57BL/6 mice. Furthermore, TM significantly increased hepatic LDLR expression and reduced plasma LDL concentrations in mice. Based on these findings, we propose a model in which ER Ca^{2+} depletion promotes the activation of SREBP2 and subsequent transcription of PCSK9. However, conditions that cause ER stress regardless of their ability to dysregulate ER Ca^{2+} inhibit PCSK9 secretion, thereby reducing PCSK9-mediated LDLR degradation and promoting LDLR-dependent hepatic cholesterol uptake. Taken together, our studies provide evidence that the retention of PCSK9 in the ER may serve as a potential strategy for lowering LDL cholesterol levels.

It is well established that the endoplasmic reticulum (ER)[3] plays a central role in the proper folding and maturation of cell surface and secretory proteins (1–3). The ability of the ER to mediate protein folding relies on the oxidative state and elevated Ca^{2+} concentration of the ER (≈400 μM) relative to the cytosol (≈100 nM) (4, 5). An equilibrium formed between ER Ca^{2+} uptake via sarco/endoplasmic reticulum ATPase and ER Ca^{2+} release mediated by two homologous classes of intracellular Ca^{2+} release channels, known as the ryanodine receptors (RYRs) and the inositol 1,4,5-triphosphate receptors, play a major role in the regulation of ER Ca^{2+} homeostasis (6). Additional regulators of ER Ca^{2+} homeostasis include ER luminal proteins that interact with Ca^{2+}, such as buffer proteins and chaperones. Many chaperones, such as calreticulin and the glucose-regulated proteins of 78 and 94 kDa (GRP78 and GRP94), can directly interact with Ca^{2+} due to the presence of Ca^{2+}-binding motifs (7–9). Other Ca^{2+}-dependent chaperones, such as protein-disulfide isomerase (PDI), interact with Ca^{2+}-bind-

* This work was supported in part by Heart and Stroke Foundation of Ontario Research Grant T-6146 (to R. C. A.), Canadian Institutes of Health Research Grant MOP-74477, the Ontario Research and Development Challenge Fund, the Canadian Institute of Health Research (to S. R. W. C.), Leducq Foundation Grant 13 CVD 03 (to N. G. S. and A. P.), Canada Research Chair 216684 (to N. G. S.), St. Joseph's Healthcare Hamilton and the Canadian Institutes of Health Research Team Grant in Thromboembolism FRN-79846. The authors declare that they have no conflicts of interest with the contents of this article.

[1] An Alberta Innovates-Health Solutions (AIHS) Scientist.

[2] Career Investigator of the Heart and Stroke Foundation of Ontario and holds the Amgen Canada Research Chair in the Division of Nephrology, St. Joseph's Healthcare and McMaster University. To whom correspondence should be addressed: 50 Charlton Ave. East, Rm. T-3313, Hamilton, Ontario L8N 4A6, Canada. Tel.: 905-522-1155 (Ext. 35175); Fax: 905-540-6589; E-mail: austinr@taari.ca.

[3] The abbreviations used are: ER, endoplasmic reticulum; TG, thapsigargin; TM, tunicamycin; LDLR, low density lipoprotein receptor; RYR, ryanodine receptor; qRT, quantitative RT; GOF, gain-of-function; LOF, loss-of-function; PDI, protein-disulfide isomerase; IHC, immunohistochemistry; INSIG, insulin-induced gene; PERK, (PKR)-like ER kinase; CHOP, CCAAT-enhancer-binding protein homologous protein; SCAP, SREBP cleavage activating protein; SREBP, sterol regulatory element-binding protein; AEBSF, 4-(2-aminoethyl)benzenesulfonyl fluoride; VLDLR, VLDL receptor; UPR, unfolded protein response; NT, untreated; PC, proprotein convertase; A23, A23187; PF, PF-429242; U18, U18666A; BAPTA, 1,2-bis(2-aminophenoxy)ethane-*N*,*N*,*N*′,*N*′-tetraacetic acid; LRP, LDLR-related protein.

ing proteins like calreticulin and therefore indirectly rely on ER Ca^{2+} (10). Overall, this intricately controlled system allows for Ca^{2+}-dependent chaperones to promote the proper folding of newly synthesized polypeptides. Any physiological conditions that alter the state of ER Ca^{2+} can impair chaperone activity, subsequently leading to an accumulation of misfolded proteins in the ER. This state, known as ER stress, contributes to hepatic injury in liver diseases such as cholestatic liver disease, alcoholic fatty liver disease, non-alcoholic fatty liver disease, and drug-induced liver disease (2, 11–13). In addition to liver disease, prolonged ER stress causes apoptosis of foam cell macrophages, thereby accelerating necrotic core formation, plaque rupture, and progression of atherosclerosis (14, 15).

Under normal physiological conditions, however, a moderate accumulation of ER luminal protein triggers the unfolded protein response (UPR), which in turn restores ER homeostasis. This highly conserved mechanism consists of three signaling cascades as follows: (*a*) the inositol-requiring protein-1α (IRE1α) with its intrinsic RNase activity splices and activates the X-box-binding protein-1 (XBP1); (*b*) the activating transcription factor-6 (ATF6); and (*c*) the protein kinase RNA (PKR)-like ER kinase (PERK), which induces the expression of proapoptotic CCAAT enhancer-binding protein homologous protein (CHOP) (1). Collectively, these UPR mediators alleviate ER stress by increasing the folding capacity of the ER and reducing the influx of newly synthesized peptides into the ER luminal space. In addition to the induction of these chaperones, we as well as others have reported that ER stress promotes the activation of the sterol regulatory element-binding protein-2 (SREBP2) (16–23). In its inactive state, SREBP2 resides in the ER through its interaction with the SREBP cleavage-activating protein (SCAP) (24) and the insulin-induced gene (INSIG) (25). Although the specific mechanism by which ER stress activates SREBP2 is unclear, it is established that low intracellular cholesterol concentrations cause release of the SCAP-SREBP2 complex from the ER anchor, INSIG (26). Upon translocation from the ER to the Golgi apparatus, SREBP2 is cleaved and activated by site-1 and -2 proteases (27–29). The active SREBP2 transcription factor then translocates to the nucleus where it up-regulates a number of genes that regulate *de novo* cholesterol synthesis or uptake (30). Among these genes (31) is the proprotein convertase subtilisin/kexin type-9 (*PCSK9*) (32), which plays a critical role in modulating cardiovascular disease (33) by blocking hepatic low density lipoprotein (LDL) cholesterol uptake and inducing the degradation of the LDL receptor (LDLR) (34–37). Despite its critical role in LDL cholesterol uptake, the precise mechanism by which ER stress activates SREBP2 and mediates LDLR and cholesterol uptake via PCSK9 has not yet been examined.

We now report that ER stress, specifically caused by ER Ca^{2+} depletion, leads to an SREBP2-dependent increase in PCSK9 expression in cultured HuH7 and HepG2 hepatocytes. In contrast, ER stress reduces circulating PCSK9 concentrations, thereby increasing cell surface hepatic LDLR expression and reducing circulating LDL concentrations. Collectively, our findings outline a novel mechanism by which ER stress modulates lipid metabolism through PCSK9.

Results

ER Ca^{2+} Depletion Induces de Novo PCSK9 Expression—To assess whether ER stress induces the expression of PCSK9, HuH7 and HepG2 cells were either untreated (NT) or treated with TG, A23187 (A23), TM, or dithiothreitol (DTT) for 24 h. Immunoblotting showed that HuH7 cells treated with agents that cause ER Ca^{2+} depletion, TG and A23, exhibit increased cellular abundance of the PCSK9 protein (Fig. 1*A*). This induction was not observed in cells treated with TM or dithiothreitol (DTT). As expected, UPR markers FLAG-sXBP1, GRP78, GRP94, and CHOP were up-regulated by all ER stress-inducing agents used. Similar results were observed in HepG2 cells (data not shown). Consistent with PCSK9 protein, PCSK9 mRNA levels were up-regulated by TG and A23 but not by TM or DTT (Fig. 1*B*), whereas all ER stress-inducing agents used increased the expression of UPR markers GRP78 and sXBP1 (*, $p < 0.05$ compared with NT). In addition, although GRP78 and sXBP1 mRNA were induced by TG within 6 h of treatment, we observed that TG did not significantly affect PCSK9 mRNA until 18 h following treatment (Fig. 1*C*; *, $p < 0.05$ compared with NT). To confirm induction of the UPR by these ER stress-inducing agents, HuH7 cells were transfected with FLAG-sXBP1 plasmid and visualized by labeling the FLAG antigen with Alexa 647 immunofluorescent secondary antibodies. Immunofluorescence images from this experiment illustrate that all ER stress-inducing agents used in our experiments induced the UPR marker FLAG-sXBP1 (Fig. 1*D*). To assess the role of ER Ca^{2+} release on PCSK9 expression, a Ca^{2+} release assay was completed in HuH7 cells using the cytosolic Ca^{2+} indicator Fura-2AM. Our data indicate that TG (*, $p < 0.05$ compared with NT) and A23 (**, $p < 0.05$ compared with NT) led to a significant increase in cytosolic Ca^{2+} (Fig. 1*E*).

In addition to the well established pharmacologic inducers of ER stress used in Fig. 1*A,* PCSK9 expression was examined following nutrient deprivation (Fig. 1*F*). Similar to our previous findings, although all conditions led to a state of ER stress, as indicated by the induction of GRP78, only those that caused a loss of ER Ca^{2+} resulted in increased PCSK9 expression. The absence of sterols also led to an induction of PCSK9, likely as a direct result of SREBP2 activation.

Given that RYRs are involved in ER Ca^{2+} homeostasis (38–41), we utilized HEK293 cells that stably overexpress mutant RYR2s to further assess the role of ER Ca^{2+} depletion on PCSK9 expression. Specifically, the gain-of-function (GOF) RYR2 mutants (Q4201R and V4653F) yield increased ER Ca^{2+} leakage, whereas the loss-of-function (LOF) RYR2 mutant (A4860G) exhibits reduced Ca^{2+} leak into the cytosol as compared with WT RYR2 (6, 42). Consistent with the effect of TG and A23, GOF RYR2 mutants induced PCSK9 expression (Fig. 1*G*). In addition, although GOF RYR2 mutants led to the up-regulation of the UPR marker CHOP, the LOF RYR2 mutation reduced GRP78 expression.

ER Ca^{2+} Depletion Induces PCSK9 Expression in an SREBP2-dependent Manner—Although SREBP2 is activated by ER stress and regulates PCSK9 expression, the link between ER stress and PCSK9 has not yet been reported. Immunoblot analysis was used to assess the effect of ER Ca^{2+} depletion on SREBP2 acti-

vation and on INSIG1 levels, a key regulator of SREBP2 activation. Both TG and A23 caused a reduction of INSIG1 while increasing the abundance of cleaved active nuclear SREBP2 (nSREBP2) (Fig. 2*A*). However, SREBP2 activation and PCSK9 expression were blocked by PF-429242 (PF), an inhibitor of site-1 proteases (Fig. 2*B*). Consistent with these findings, blocking the activation of SREBP2 with PF as well as fatostatin or AEBSF significantly reduced the expression of PCSK9 at the mRNA level (Fig. 2*C*; #, $p < 0.05$ compared with NT). TG-induced PCSK9 expression (*, $p < 0.05$ compared with NT) was

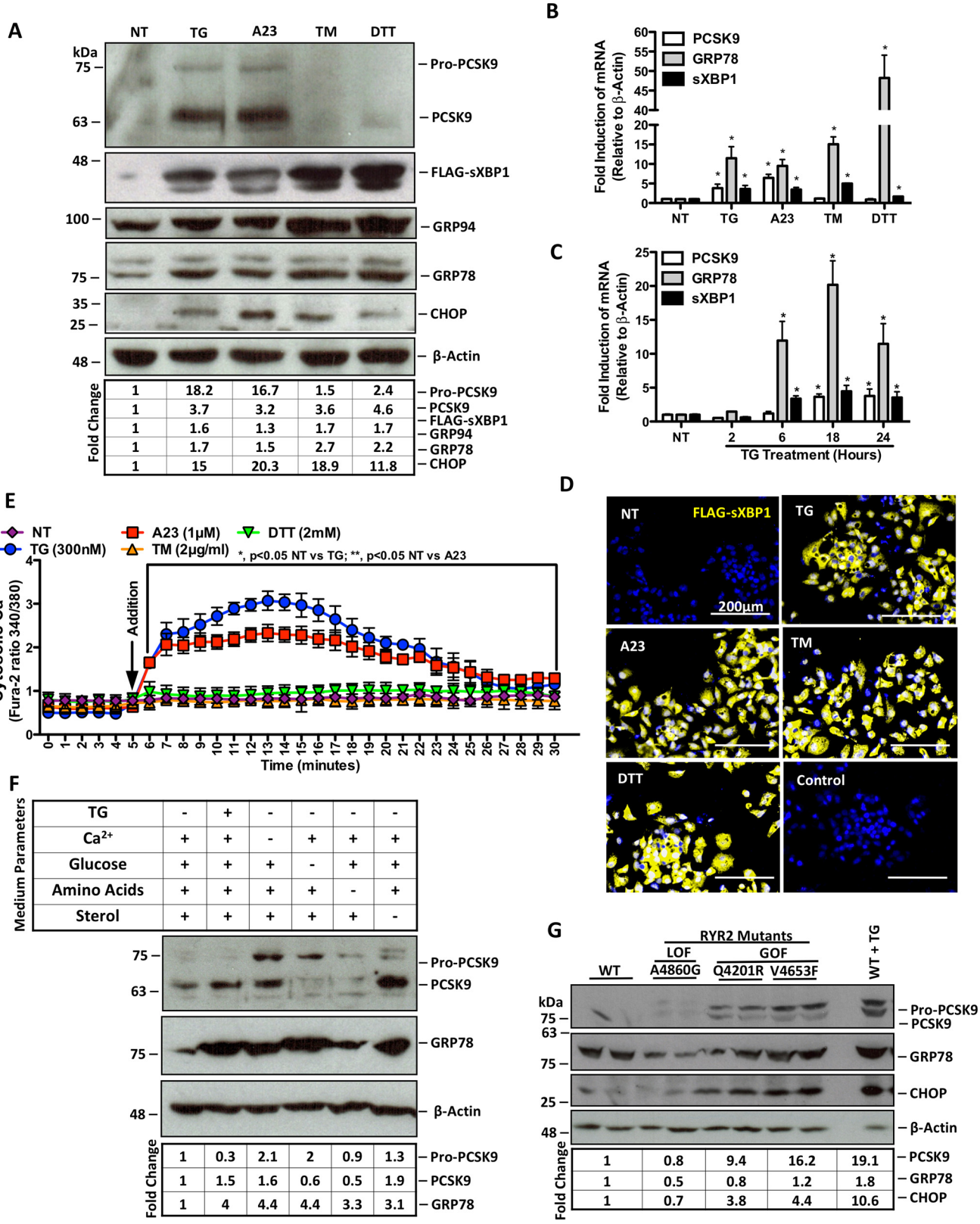

also blocked by these agents ($, $p < 0.05$ compared with TG). In a manner consistent with Fig. 2, *B* and *C*, treatment of cells with siRNA knockdown of SREBP2 blocked TG-mediated PCSK9 induction to a similar extent as that observed for U18666A (U18), a known activator of SREBP2 (Fig. 2*D*) (43).

In support of these findings, we confirmed the link between SREBP2 activation and PCSK9 expression in our model by promoting the activation of SREBP2. Similar to Fig. 2*D*, the treatment of HuH7 cells with U18 led to the activation of SREBP2 and a subsequent increase in the expression of downstream targets PCSK9 and LDLR without affecting UPR markers GRP94 and CHOP (Fig. 2*E*). Consistent with our SREBP2 inhibition studies, RT-PCR data also showed that PF (**, $p < 0.05$ compared with U18) can block U18-induced (*, $p < 0.05$ compared with NT) PCSK9 expression (Fig. 2*F*). To examine whether U18, which induces SREBP2 activation via sterol starvation, also causes ER Ca^{2+} release, a cytosolic Ca^{2+} release assay was completed. These data show that U18 causes a robust activation of SREBP2 without a spontaneous loss of ER Ca^{2+} (Fig. 2*G*).

ER Stress Reduces PCSK9 Secretion—Given that the interaction between PCSK9 and the LDLR occurs primarily in the extracellular space of the hepatocyte, we explored the effect of ER stress on PCSK9 secretion. Using ELISAs, we found that TG and TM significantly reduced the levels of secreted PCSK9 within the media from HuH7 cells (Fig. 3*A*, *, $p < 0.05$ compared with NT). Furthermore, TM reduced secreted PCSK9 concentrations to a significantly greater extent than TG (Fig. 3*A*, ±, $p < 0.05$ compared with TG). Similar results were observed in mouse primary hepatocytes (Fig. 3*B*). Given that TG increases the mRNA and cellular abundance of PCSK9, yet blocks its secretion, we next aimed to assess whether TG causes intracellular PCSK9 accumulation. HuH7 cells were pretreated with TG and subsequently permitted to rest in fresh TG-free media for 48 h. Secreted PCSK9 concentrations from the 24 to 48-h period following pretreatment were significantly greater than that of untreated cells (Fig. 3*C*). To explore the link between SREBP2 and secreted PCSK9, the media from AEBSF- and PF-treated HuH7 cells was also examined and found to contain significantly less PCSK9 than untreated controls (Fig. 3*D*, *, $p < 0.05$ compared with NT).

To determine the correlation between ER stress and PCSK9 secretion, HuH7 cells were treated with increasing concentrations of TM for 24 h. GRP78 protein expression, which served as a marker of UPR activation, was compared with the PCSK9 content in the media (Fig. 3*E*). A Pearson's correlation analysis of these data showed that the induction of the UPR inversely correlates with PCSK9 secretion ($r = -0.871$, $p = 0.0005$), which is significant (Fig. 3*E*,*, $p < 0.05$) at doses higher than 0.06 μg/ml TM.

ER Stress Retains PCSK9 in the ER—Given our previous findings that ER Ca^{2+} depletion induces *de novo* expression and cellular abundance of PCSK9, yet blocked its secretion, the cellular localization of TG- and TM-induced PCSK9 accumulation was examined. HuH7 cells transfected with V5-labeled PCSK9 were stained initially with rhodamine phalloidin and PDI to visualize the cytoskeleton and ER, respectively (Fig. 4*A*). Transfected cells were also stained for V5 and PDI (Fig. 4*B*). Upon analysis of these cells, we first observed that ER stress, whether induced by TG or TM, appeared to increase the relative size of the ER, an established phenomenon known as ER expansion (44). In addition, V5 staining revealed that PCSK9 remains confined to the ER irregardless of conditions that cause ER stress (Fig. 4). Collectively, these data indicate that regardless of the status of the UPR, exogenously expressed PCSK9 predominantly resides in the ER, as reported previously for WT PCSK9 (45).

TM Blocks PCSK9 Secretion and Induces Hepatic Cell Surface LDLR Expression in Vivo—To explore the effect of ER stress on PCSK9 secretion *in vivo*, C57BL/6 female mice were treated with increasing concentrations of TM for 24 h (Fig. 5*A*) or given a single treatment and sacrificed at 24-h intervals for a total of 120 h (Fig. 5*B*). Consistent with our *in vitro* findings, plasma PCSK9 levels were significantly reduced following TM treatment. This inhibitory effect of TM on plasma PCSK9 levels occurred at all doses of TM (*, $p < 0.05$), in a dose-dependent manner (±, $p < 0.05$) and persisted for up to 120 h following injection of TM (#, $p < 0.05$). Because of the role of PCSK9 as a major regulator of hepatic LDLR, we also examined LDLR expression. LDLR-stained liver sections from these animals show that TM induced hepatic cell surface LDLR to a similar extent as those observed in the well described PCSK9 KO mice (Fig. 5*C*) (46). The quantification of sections from multiple animals ($n = 3$) reveals similar results (Fig. 5*D*, *, $p < 0.05$). LDLR histology findings were confirmed using immunoblots, and as expected, ER stress markers GRP78 and CHOP were up-regulated by TM along with the LDLR (Fig. 5*E*). Non-permeabilized mouse primary hepatocytes were also stained for LDLR to confirm the cell surface localization of TM-dependent LDLR expression (Fig. 5*F*). Taken together, these data suggest that blockage of PCSK9 secretion, via ER stress, up-regulates hepatic LDLR expression.

TM Reduces the LDL Cholesterol Content of Plasma—Given the effect of ER stress on hepatic PCSK9 retention and

FIGURE 1. **ER Ca^{2+} depletion induces *de novo* PCSK9 expression.** HuH7 cells were seeded in DMEM and transfected with the FLAG-sXBP1 ER stress reporter plasmid. Cells were subsequently untreated (*NT*) or treated with ER stress-inducing agents TG (100 nM), A23 (1 μM), TM (2 μg/ml), or DTT (2 mM) for 24 h. *A* and *B*, following treatment, protein lysates were collected for immunoblot analysis of PCSK9 and UPR markers FLAG-sXBP1, GRP94, GRP78, and CHOP. RNA was collected for qRT-PCR analysis of PCSK9, sXBP1, and GRP78. *C*, RNA from HuH7 cells treated with TG (100 nM) for 2, 6, 18, or 24 h were also examined via qRT-PCR to determine the time dependence of TG-induced PCSK9 expression. *, $p < 0.05$. *D*, HuH7 cells, which underwent the same transfection and treatment conditions as in *A* and *B*, were also stained for FLAG to examine UPR induction via immunofluorescence microscopy. *E*, HuH7 cells were plated in clear bottom 96-well plates and incubated with Fura-2AM, a fluorescent cytosolic Ca^{2+} indicator, for 30 min. Following incubation, cytosolic Ca^{2+} of cells treated with ER stress-inducing agents was measured for 30 min. *F*, to determine the effect of ER stress-inducing conditions via non-pharmacologic means on PCSK9 expression, HuH7 cells were exposed to medium deficient in either Ca^{2+}, glucose, amino acids, or sterol for 24 h. *G*, in addition, the role of ER Ca^{2+} loss on PCSK9 expression was examined using HEK293 cells that stably overexpress tetracycline-inducible GOF or LOF RYR2 mutants using immunoblots. GOF RYR2 mutant cell lines (Q4201R and V4653F) exhibit increased ER Ca^{2+} leakage, whereas LOF RYR2 mutant (A4860G) exhibits reduced ER Ca^{2+} leak compared to WT cells (6, 42). Differences between treatments were assessed with paired Student's *t* tests, and all values are represented as mean ± S.D.

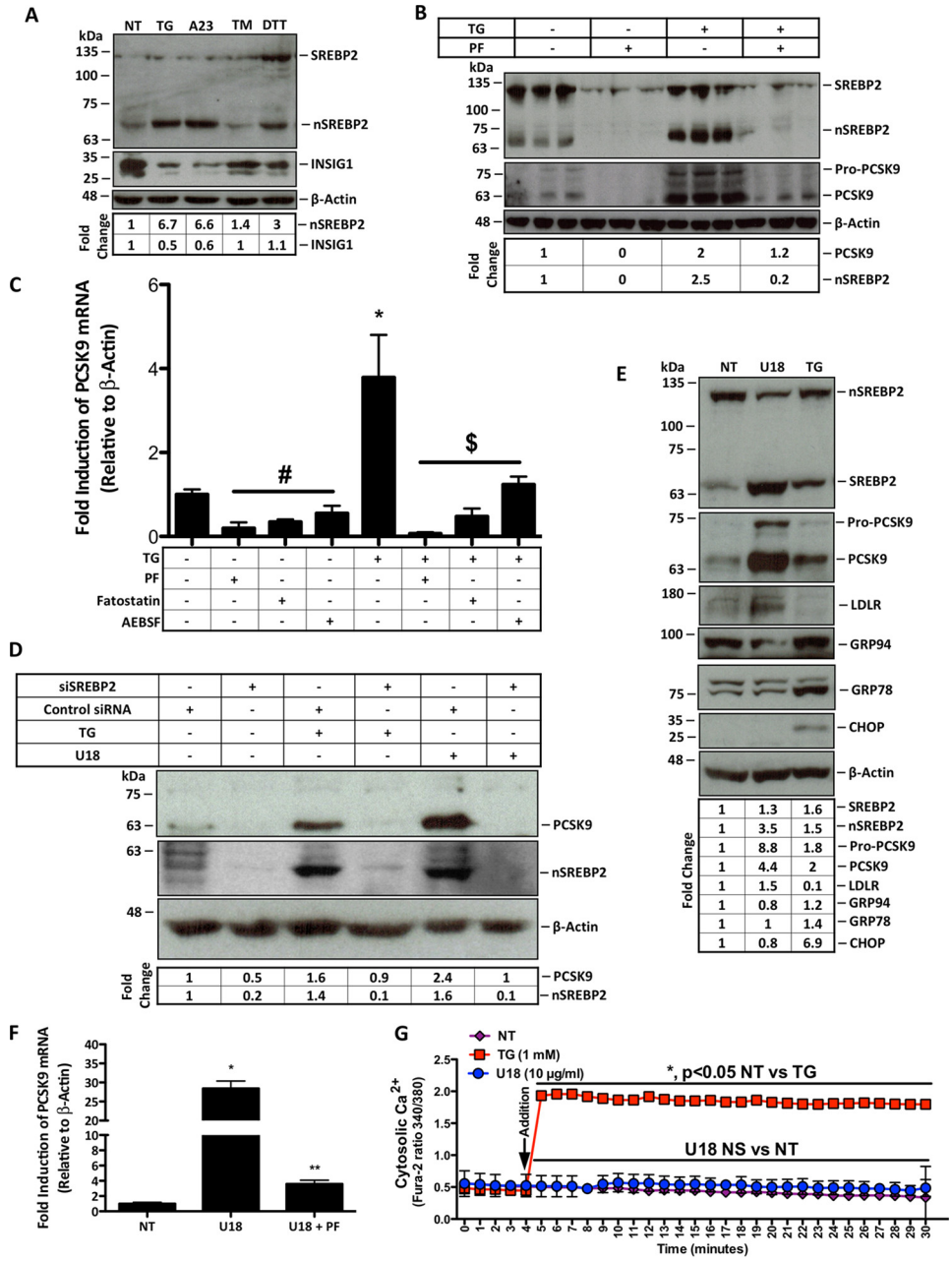

FIGURE 2. **ER Ca^{2+} depletion induces PCSK9 expression in an SREBP2-dependent manner.** *A*, protein lysates were collected from HuH7 cells either untreated (*NT*) or treated with ER stress-inducing agents TG (100 nM), A23 (1 μM), TM (2 μg/ml), or DTT (2 mM) for 24 h for immunoblot analysis. *B*, HuH7 cells were then treated with TG in the presence or absence of PF (10 μM), which inhibits SREBP2 activation, for 24 h. Immunoblot analysis was carried out as in *A* to examine the SREBP2 dependence of PCSK9 expression resulting from ER Ca^{2+} release. *C*, RNA was collected from HuH7 cells, which were treated with additional inhibitors of SREBP2 activation, including AEBSF (0.3 mM) and fatostatin (20 μM) in the presence or absence of TG (100 nM) to further elucidate the SREBP2 dependence of PCSK9 expression. #, $p < 0.05$ *versus* untreated cells (*NT*); *, $p < 0.05$ *versus* NT; $, $p < 0.05$ *versus* TG-treated cells. *D*, to confirm the link between SREBP2 activation and PCSK9 expression in our model, HuH7 cells were transfected with SREBP2 siRNA. Following transfection, cells were also treated with TG (100 nM) or U18 (1 μg/ml), an inducer of SREBP2 activation, for 24 h. *E*, to examine SREBP2 activation by U18, immunoblots were used to directly assess SREBP2 and markers of SREBP2 activation, PCSK9 and LDLR; UPR markers GRP94, GRP78, and CHOP were also evaluated to determine the influence of U18 on UPR activation. *F*, PCSK9 mRNA was also examined in HuH7 cells treated with U18 in the presence or absence of PF for 24 h. *, $p < 0.05$ *versus* NT; **, $p < 0.05$ *versus* U18-treated cells. *G*, to assess whether U18-induced PCSK9 expression occurs in a Ca^{2+}-dependent manner, HuH7 cells were incubated with fluorescent cytosolic Ca^{2+} indicator for 30 min and subsequently treated with U18 (10 μg/ml) or TG (1 mM) control. Differences between treatments were assessed with paired Student's *t* tests, and all values are represented as mean ± S.D.

increased LDLR expression, we next aimed to delineate the functional implications of these observations on circulating cholesterol levels. Our findings showed that TM treatment significantly reduces total plasma cholesterol (Fig. 6*A*, *, $p < 0.05$) and triglycerides (Fig. 6*B*, *, $p < 0.05$). Immunoblotting revealed that TM also significantly reduced the serum levels of apolipoprotein (apo) B100 and apoB48 (Fig. 6*C*) suggesting reduced abundance of very low density lipoprotein (VLDL) and LDL particles (47). Importantly, hepatic UPR markers GRP94, GRP78, and IRE1-α all confirm that TM treatment was successful in causing hepatic ER stress. Fast protein liquid chromatography (FLPC) cholesterol profile of the TM-treated mice

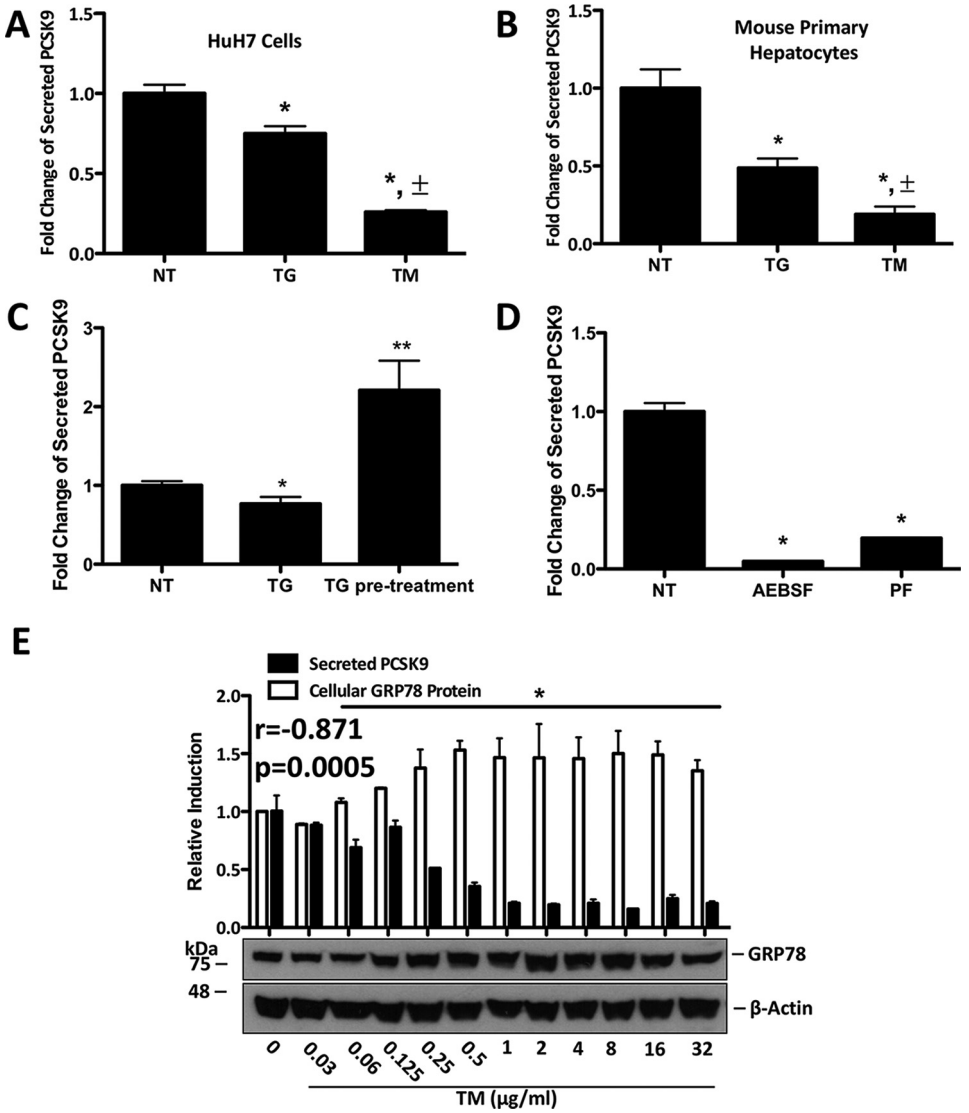

FIGURE 3. **ER stress reduces PCSK9 secretion.** *A* and *B*, HuH7 cells and primary hepatocytes were either untreated (*NT*) or treated with TG (100 nM) or TM (2 μg/ml) for 24 h. The FBS-free medium, in which these cells were cultured and treated, was collected and examined for secreted PCSK9 via ELISAs. *A* and *B*, $\pm$, $p < 0.05$ *versus* TG-treated cells. *C*, secreted PCSK9 was then examined in the media of HuH7 cells, which were pretreated with TG (100 nM) for 4 h and permitted to rest in TG-free medium for 48 h. *D*, to examine the effect of SREBP2 inhibition on secreted PCSK9, FBS-free medium from HuH7 cells treated with AEBSF (0.3 mM) was also examined via ELISAs. *A–D*, *, $p < 0.05$ *versus* non-treated cells (*NT*). **, $p < 0.05$ *versus* TG-treated cells. *E*, correlation between UPR activation and PCSK9 secretion was assessed using a dose-response experiment in which HuH7 cells were treated with increasing concentrations of TM for 24 h. GRP78 expression, determined via immunoblots, was quantified and compared with ELISA data generated from the medium of the respective HuH7 cells. A Pearson's correlation was used to establish the relationship between cellular GRP78 expression and secreted PCSK9 ($r = -0.871$, $p = 0.0005$). *E*, $p < 0.05$ *versus* NT. Differences between treatments were assessed with paired Student's *t* tests, and all values are represented as mean $\pm$ S.D.

showed the cholesterol-lowering effect of TM (Fig. 6*D*). Quantification of these lipid profiles confirmed that TM significantly reduced plasma cholesterol concentrations in all lipoprotein classes (Fig. 6*E*; *, $p < 0.05$). These data demonstrate that TM has a potent cholesterol-lowering effect *in vivo*.

Discussion

In this study, we identify a novel role for ER stress in the modulation of hepatic PCSK9 and LDLR. We observed a striking consistency in our *in vitro* data, using a variety of cell lines, with respect to the up-regulation of PCSK9 in response to ER stress conditions that cause ER Ca^{2+} depletion (Fig. 1). In addition to the up-regulation of PCSK9 by TG and A23, a similar observation was made using sarco/endoplasmic reticulum ATPase inhibitors cyclopiazonic acid (1 μM) and cyclosporin-A (10 μg/ml) (data not shown). Previous pulse-chase studies have reported that TG- and A23-mediated ER Ca^{2+} depletion for up to 4 h had no effect on the zymogen processing or Tyr sulfonation of PCSK9 (32), which allow for its maturation and secretion, respectively. In accordance with this observation, our findings suggest that the effect of ER Ca^{2+} depletion on endogenous PCSK9 has no direct effect on PCSK9 processing. Rather, we observed a distinct effect of ER Ca^{2+} depletion on the transcriptional regulation of endogenous PCSK9 via Ca^{2+}-dependent SREBP2 activation. Notably, the observed activation of SREBP2 that we observed may be caused by the down-regulation of INSIG1 expression (Fig. 2*A*). A recent report in which copper-induced ER stress leads to ER Ca^{2+} depletion and sub-

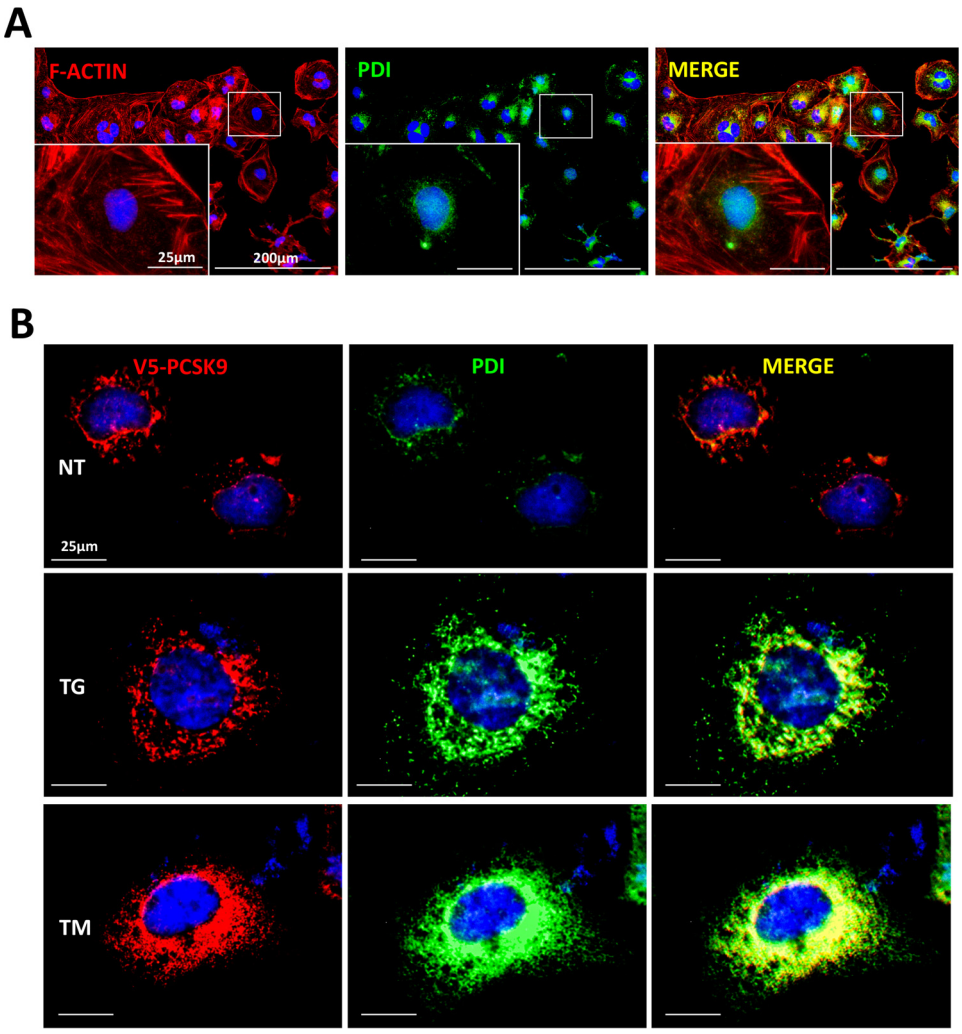

FIGURE 4. **ER stress retains PCSK9 in the ER.** HuH7 cells were plated in chamber slides and transfected with V5-PCSK9. Cells were subsequently either untreated (*NT*), treated with TG (100 nM), or TM (2 μg/ml) for 24 h. *A*, cells were then fixed and stained with rhodamine phalloidin (*red*) and ER marker PDI to allow for visualization of the cellular location of the ER relative to the cytosol. *B*, in addition, cells were also stained for V5 and PDI to identify the cellular localization of PCSK9. PCSK9 (*red*) was visualized using Alexa 594 fluorescent secondary antibodies, whereas PDI (*green*) was visualized using Alexa 647 fluorescent secondary antibodies.

sequent reduction in INSIG expression lends support to our findings (48). In addition, it has been shown that the down-regulation of an ER-resident Ca^{2+}-binding protein, calreticulin, results in ER Ca^{2+} loss and increased SREBP-1C activation (23). Finally, the direct effect of TG on the activation of SREBP-1 and -2 has also been reported previously (21). In addition to these findings, these authors also demonstrated that the TG-mediated activation of SREBP could be reversed with a 6-h treatment of the Ca^{2+}-chelating agent BAPTA (21). However, the effect of BAPTA on cellular Ca^{2+} homeostasis is subjected to temporal variations. Upon treatment of HuH7 cells with BAPTA for 24 h, we observed increased PCSK9 expression similar to that of the effect of TG (data not shown). This likely occurred due to excessive cytosolic Ca^{2+} chelation resulting in ER Ca^{2+} depletion. Furthermore, as a consequence of causing ER Ca^{2+} depletion by blocking ER Ca^{2+} uptake, TG increases cytosolic Ca^{2+} content. For this reason, the induction of PCSK9 via a 24-h treatment of BAPTA indicates that TG-mediated PCSK9 expression occurs primarily as a result of ER Ca^{2+} depletion and is not due to increased cytosolic Ca^{2+}. Collectively, our findings, as well as those of others, support a model in which a spontaneous loss of ER Ca^{2+} promotes the activation of SREBP2 and a consequent up-regulation of PCSK9. However, the specific mechanism by which ER Ca^{2+} depletion causes the down-regulation of INSIG1 and release of SREBP2 from the ER remains to be elucidated.

We also explored the effect of ER stress on PCSK9 secretion in cultured HuH7 cells and mouse primary hepatocytes. Given our previous findings that TG increased PCSK9 expression, we measured PCSK9 in the media from these cells. We found that ER stress, whether induced by TG or TM, significantly reduced the PCSK9 content of media (Fig. 4, *A* and *B*). In addition, PCSK9 appears to accumulate in the cell during conditions of stress and is subsequently processed and secreted upon alleviation of such conditions (Fig. 4*C*). Consistent with these findings, TM-treated mice also had significantly less circulating PCSK9 (Fig. 5*A*). The mechanism by which ER stress reduces PCSK9 in the media/plasma remains unclear. However, because these agents fail to block the autocatalytic cleavage of PCSK9 from its premature (75 kDa) to its mature form (68 kDa)

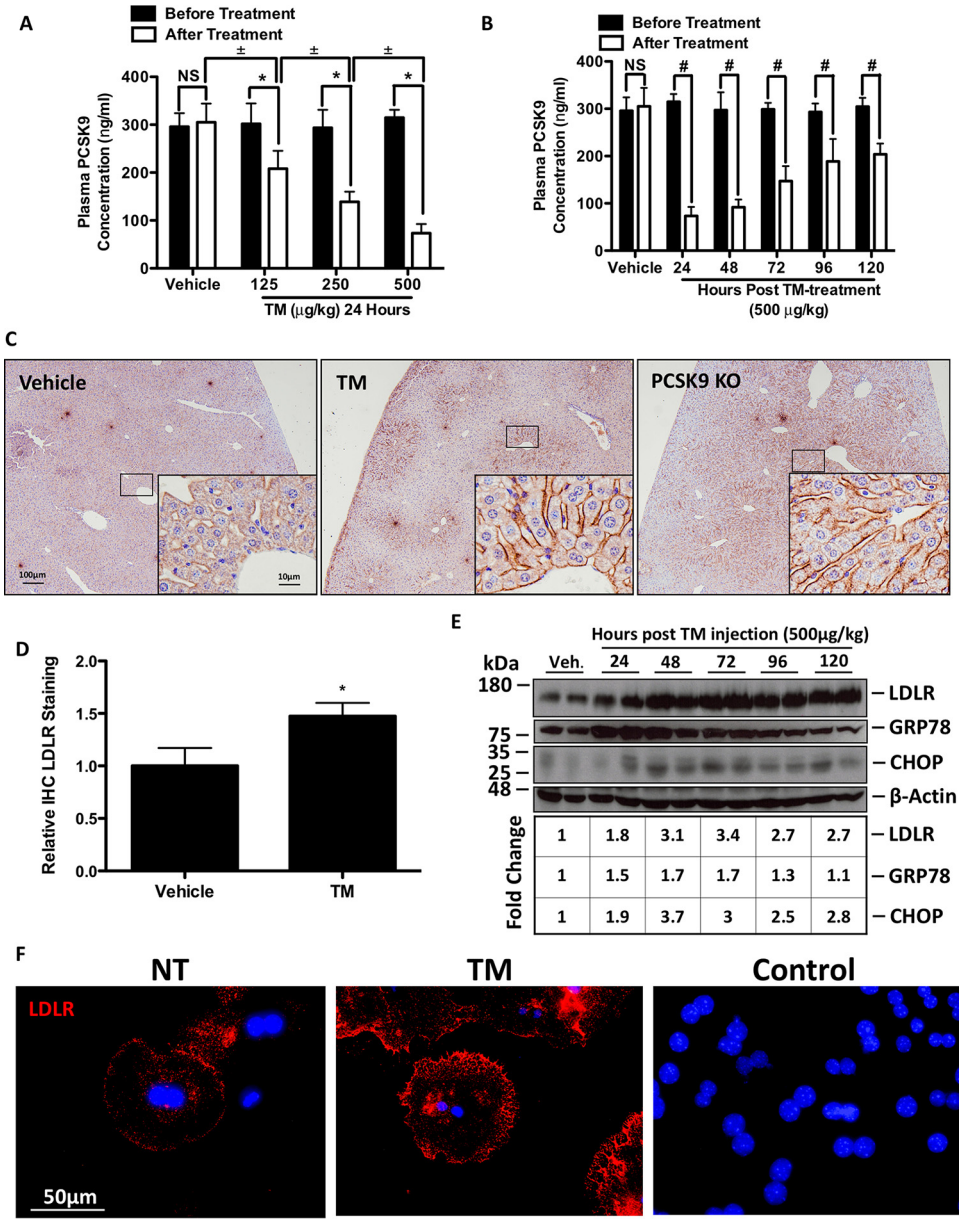

FIGURE 5. **TM blocks PCSK9 secretion and induces hepatic cell surface LDLR expression *in vivo*.** 12-Week-old C57BL/6 female mice were randomly divided into eight groups ($n = 3$) and subcutaneously injected with a single dose of PBS vehicle control or TM. Animals treated with PBS or TM (125–500 μg/kg) were sacrificed 24 h following injection. The remaining animals, belonging to groups 5–8 were treated with a single injection of TM (500 μg/kg) and sacrificed every 24 h for the following 120 h. Plasma was taken from each mouse prior to injection and after sacrifice. *A*, *, $p < 0.05$ *versus* before treatment. ±, $p < 0.05$ *versus* after treatment. *A* and *B*, plasma PCSK9 levels were quantified via ELISAs. *B*, #, $p < 0.05$ *versus* before treatment. *C* and *D*, livers from the TM-treated and untreated PCSK9 KO mice were collected, fixed in formalin, sectioned, stained for LDLR, and quantified. *E*, flash-frozen liver tissues from these animals were used to examine the expression of LDLR and of UPR markers GRP78 and CHOP using immunoblots. *, $p < 0.05$ *versus* vehicle. *F*, to elucidate whether IHC LDLR stating occurred specifically on cell surface LDLR, mouse primary hepatocytes were plated and stained for LDLR in the absence of permeabilizing agents. *Control*, HuH7 cells were also incubated with Alexa 594 secondary antibody, in the absence of primary antibody staining. Differences between treatments were assessed with unpaired Student's *t* tests, and all values are represented as mean ± S.D. *Veh*, vehicle; *NS*, not significant.

(Fig. 1*A*), our data suggest that ER stress does not directly affect PCSK9. Rather, ER stress is likely affecting other proteins in the PCSK9 secretory pathway. Recent reports have identified GRP94, an ER stress inducible protein, as an ER-resident binding partner of PCSK9 (49). Furthermore, it has been shown that the exit of PCSK9 from the ER depends on anterograde COPII vesicular trafficking (50), a process known to be impaired by ER stress (51). Taken together, these findings suggest that ER stress increases the PCSK9-retaining ability of the ER (Fig. 3) by up-regulating GRP94 (Figs. 1*A* and 6*C*), and it further hinders the exit of PCSK9 from the ER by blocking COPII vesicular transport.

Consistent with our findings, it has been reported that circulating PCSK9 levels were significantly reduced in mice fed a high cholesterol diet (52), a condition known to cause hepatic UPR activation (53). Most notably however, the reduction in circulating PCSK9 levels was linked to an increase in hepatic LDLR expression.

Similar to previous reports, we found plasma PCSK9 concentrations to be inversely related to hepatic cell surface LDLR

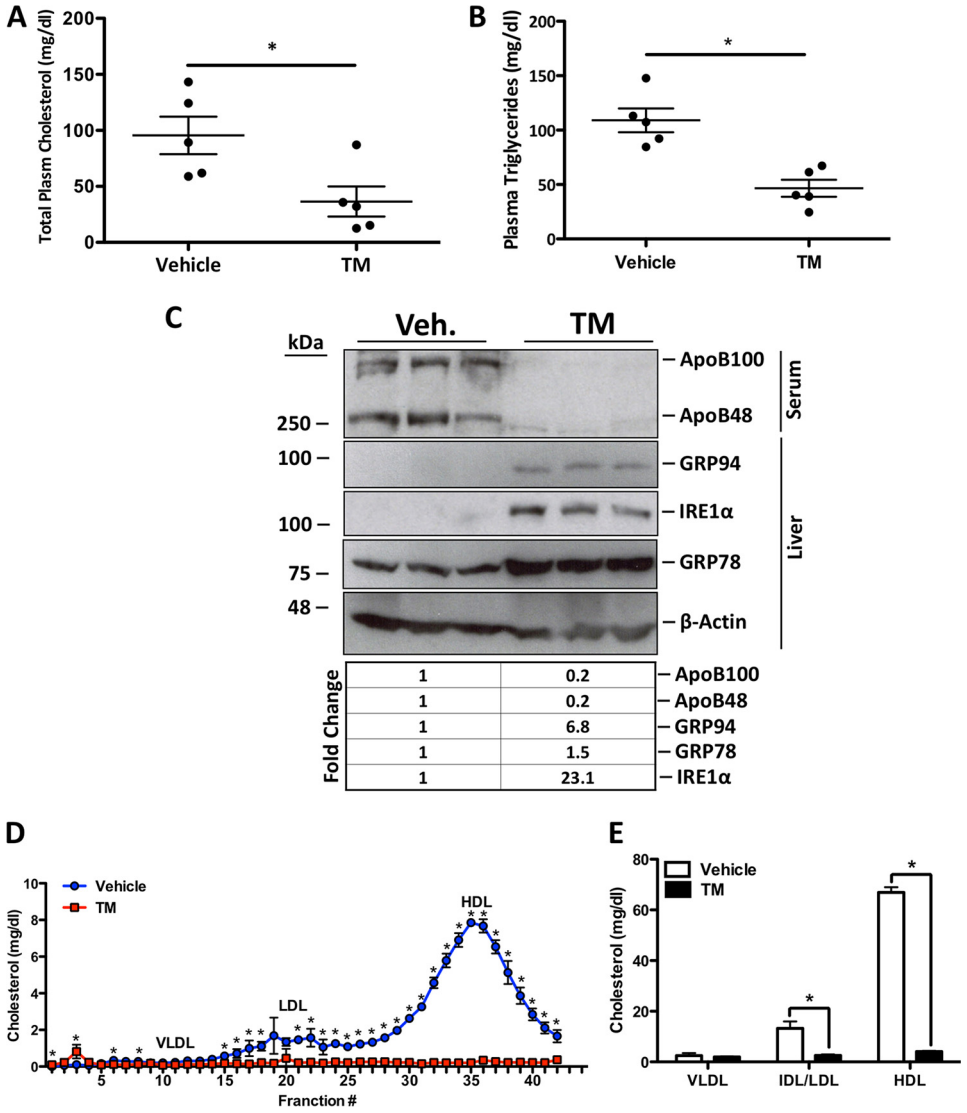

FIGURE 6. **Tunicamycin reduces the LDL cholesterol content of plasma.** 12-Week-old C57BL/6 female mice were subcutaneously injected with a single dose of TM (500 μg/kg) and sacrificed 24 h later. *A* and *B*, plasma was collected after sacrifice and total cholesterol and triglycerides were quantified using enzymatic assays. *A* and *B*, *, $p < 0.05$ *versus* vehicle. *C*, to determine the effect of TM on LDL cholesterol, plasma apoB48 and apoB100 were examined using immunoblots. Immunoblot analysis was also used to ensure TM-mediated induction of UPR markers GRP94, GRP78, and IRE1α. *D*, to further elucidate the effect of TM on all lipoprotein fractions, FPLC analysis was used to construct a lipid profile. Differences between treatments were assessed with paired Student's *t* tests, and all values are represented as mean ± S.D. *E*, *, $p < 0.05$ *versus* vehicle (NT). *Veh,* vehicle.

expression (37, 54, 55). Although it has been reported that TM induces the VLDLR via the PERK-ATF4 pathway (13), the potential mechanisms by which TM affects LDLR expression are numerous. First, because of the glycosylated nature of the LDLR, the direct impact of TM, which inhibits *N*-glycosylation, on the LDLR must be taken into consideration. Upon longer exposure of our LDLR immunoblots (Fig. 5*E*), it became apparent that TM caused a distinct accumulation of premature non-*N*-glycosylated LDLR (120 kDa, data not shown) in the livers of these mice. For this reason, the increase in LDLR expression, however, is likely a result of increased LDLR half-life due to the TM-mediated loss of PCSK9 in circulation.

Alternatively, it has been reported that newly synthesized mature ER-resident PCSK9 can act as a chaperone of the LDLR, thereby contributing to LDLR maturation and exit from the ER (56). Based on these findings, and given the effect of TM on ER PCSK9 retention (Fig. 4), it is also possible that the abundance of PCSK9 in the ER leads to a net increase in PCSK9-mediated ER LDLR processing and maturation.

Finally, although LDLR expression is transcriptionally regulated by SREBP2 (57), which can be activated by ER stress (2, 11–13), our data indicate that ER Ca^{2+} release is necessary for this process to occur (Fig. 2*A*). Based on these findings, it is unlikely that TM is directly inducing hepatic cell surface LDLR expression via SREBP2 activation. Consistent with this, others have determined that TM blocks the *N*-glycosylation and stability of SCAP, leading to a reduction of SREBP1/2 activation (58).

In addition to association between the loss of circulating PCSK9 and elevated LDLR expression, we also describe a TM-mediated ablation of circulating LDL (Fig. 6, *C*–*E*). Others have reported that TM blocks *de novo* cholesterol synthesis via direct inhibition of 3-hydroxy-3-methylglutaryl-coenzyme A reductase (59) and reduces cholesterol efflux (60). However, a model

in which TM reduces circulating LDL via LDLR has not been reported.

Moreover, we also observed a significant reduction in circulating HDL levels (Fig. 6, *D* and *E*). This finding has been described previously, in which lower circulating HDL levels in PCSK9$^{-/-}$ mice were shown to be dependent on LDLR-mediated uptake of HDL via apoE (61). It is also established that other ER stress-inducible members of the LDLR family, including the LDLR-related protein (LRP) (62) and VLDLR (13), can bind and internalize apoE-containing HDL (63) and be degraded by circulating PCSK9 (64–67). Consistent with these findings, the overexpression of profurin, the prodomain of a member of the proprotein convertase (PC) family, blocks PC activation and subsequently abrogates circulating HDL levels (68). Based on our findings, as well as those mentioned herein, TM may be reducing circulating HDL levels by inducing the expression of apoE-binding receptors such as the LDLR (Fig. 5*C*), VLDLR (13), and LRP. Furthermore, in a manner similar to profurin, the inhibition of *N*-glycosylation by TM may also be affecting PC activation thereby further contributing to the reduction in circulating HDL levels.

Currently, the mechanism by which PCSK9 is secreted remains unclear. However, in agreement with other studies, our findings demonstrate that PCSK9 secretion is a highly regulated process potentially involving multiple cellular pathways (63, 69–71). Our studies show that inhibition of *N*-glycosylation and induction of the UPR markedly impairs PCSK9 secretion. Our data further support the notion that reducing PCSK9 secretion, via ER retention, may contribute to a reduction in circulating LDL cholesterol (72). Overall, this study further enforces the need for additional investigations to delineate the mechanism(s) by which ER Ca^{2+} and ER stress play a role in the expression and cellular retention of PCSK9.

Experimental Procedures

Cell Culture and Cell Treatment—Human hepatocellular carcinoma HuH7 and HepG2 cells were chosen because they are known to express and secrete PCSK9 (73, 74). HuH7 cells were a generous gift from Dr. Nabil G. Seidah (University of Montreal), and HepG2 cells were purchased from American Type Culture Collection (catalog no. HB-8065). HuH7 cells and HepG2 cells were routinely grown at 37 °C with 5% CO_2 in Dulbecco's modified Eagle's medium (DMEM) (Gibco, Thermo Fisher Scientific, Waltham, MA) containing 10% fetal bovine serum (FBS, Sigma), 100 IU/ml penicillin, and 100 μg/ml streptomycin (Gibco, Thermo Fisher Scientific). HEK293 cells overexpressing RYR2 mutants (75) were used to examine PCSK9 expression. Briefly, HEK293 cells were plated to a confluence of 90% in DMEM containing 10% FBS, 100 IU/ml penicillin, 100 μg/ml streptomycin, 4 mM L-glutamine (Sigma), 0.1 mM nonessential amino acids (Gibco, Thermo Fisher Scientific), and expression of RYR2 wild type (WT) and mutants was induced via incubation with tetracycline (1 μg/ml, Sigma) for 24 h (76). Cells were subsequently treated with agents that induced varying types of ER stress for 24 h. TG (100 nM, Sigma), and Ca^{2+} ionophore A23 (1 μM, Sigma) cause ER Ca^{2+} depletion (32); TM (2 μg/ml, Sigma) inhibits *N*-glycosylation (77), and the reducing agent DTT (2 mM, Sigma) disrupts disulfide bond formation by compromising the oxidative environment of the ER lumen (18). To further examine the conditions of ER stress on PCSK9 expression, HuH7 cells were incubated in medium deficient in either Ca^{2+} (catalog no. 21068-028, Gibco, Thermo Fisher Scientific), D-glucose (catalog no. 11966-025, Gibco, Thermo Fisher Scientific), amino acids (catalog no. 24010-043, Gibco, Thermo Fisher Scientific), or sterols. With the exception of the medium deficient in sterol, which contained no FBS, all media used in these experiments were supplemented with dialyzed FBS (catalog no. 26400-036, Gibco, Thermo Fisher Scientific). To block the activation of SREBP2, cells were treated with AEBSF (20) (0.3 mM, Sigma), fatostatin (78) (20 μM, Sigma), or PF (10 μM, Sigma) (79) for 24 h. siRNA was also used to block SREBP2; briefly, HuH7 cells were transfected with SREBP2 siRNA (catalog no. 4390824, Thermo Fisher Scientific) or control siRNA (catalog no. 4390843, Thermo Fisher Scientific) using Lipofectamine RNAiMAX (catalog no. 13778030, Thermo Fisher Scientific) and incubated in the transfection mixture for 48 h. Cells were then either untreated or treated with TG (100 nM) or U18 (1 μg/ml, Sigma) for 24 h following initiation of the transfection. In addition to TG, U18 was used as an activator of SREBP2 due to its ability to promote intracellular sterol starvation (43).

Hepatocyte Isolation—Primary hepatocytes were isolated from 12-week-old male C57BL/6 mice in a two-step hepatic perfusion of prewarmed EGTA (500 μM in HEPES buffer, Sigma) and collagenase (0.05% in HEPES buffer, Sigma) solutions (80). Immediately proceeding the harvest, cells were washed, collected via low speed centrifugation with cell strainers, and plated (10^6 cells/ml) in warm William's E medium (Gibco, Thermo Fisher Scientific) supplemented with 10% FBS, 100 IU/ml penicillin, and 100 μg/ml streptomycin.

Measurement of Intracellular Ca^{2+}—Intracellular Ca^{2+} in HuH7 cells was measured using the Fura-2AM fluorescent indicator as described previously (81). Briefly, cells were plated in clear-bottom white 96-well plates (Nunc, Denmark) to a confluence of 80%. Following a 24-h resting period, cells were washed and incubated with Fura-2AM (2 μM) for 30 min. Cells were subsequently washed again and left to incubate in Hanks' balanced salt solution containing 10 mM HEPES during the course of the experiment. Fluorescence intensity measurements were taken every minute for 30 min at two distinct wavelengths (excitation 340/emission 515 and excitation 380/emission 515) using a SpectraMax Gemini EM fluorescent spectrophotometer (Molecular Devices, Sunnyvale, CA).

Plasmids, Transfections, and Immunofluorescence Microscopy—To ensure appropriate induction of the UPR by the ER stress-inducing agents used, HuH7 cells were transfected with an ER stress-activated indicator plasmid as described previously (82). Briefly, under conditions of stress, the ER stress-specific intron is spliced and removed from the ER stress-activated indicator mRNA transcript leading to a frameshift and subsequent production of functional FLAG-spliced XBP1 (sXBP1) protein. ER stress-induced FLAG-sXBP1 was visualized by staining for FLAG. To determine the cellular localization of PCSK9 in conditions of stress, HuH7 cells were transfected with WT V5-labeled PCSK9, as described previously (83), and stained for V5. Transfection of the HuH7 cells with

this plasmid was performed at 60% confluence. Briefly, a transfection mixture consisting of a 1:3 ratio (2 μg, 6 μl) of plasmid/X-tremeGENE (catalog no. 6366236001 Roche Applied Science and Sigma) and 192 μl of Opti-MEM (Thermo Fisher Scientific) were added to the HuH7 cells in 6-well culture dishes or 4-well chamber slides (catalog no.177399, Thermo Fisher Scientific) containing complete DMEM for 48 h. ER stress-inducing agents were added 24 h after the addition of the transfection mixture. Cells were either lysed for immunoblot analysis or fixed with 4% paraformaldehyde for immunofluorescence microscopy. Fixed cells were subsequently washed with PBS, either non-permeabilized or permeabilized with 0.025% Triton-X in 1× PBS, and blocked with 1% bovine serum albumin for 30 min. Cells were then stained with anti-FLAG (catalog no. F3040 Sigma), anti-V5 (catalog no. sc-83849, Santa Cruz Biotechnology), anti-LDLR (catalog no. AF2255, R&D Systems), or anti-PDI (catalog no. C81H6, Cell Signaling Technology) for 1 h in 1% BSA in 1× PBS-T. Following incubation with primary antibody, cells were washed and incubated with either Alexa 594 (catalog no. A11058, Thermo Fisher Scientific) or Alexa 647 (catalog no. 21245, Thermo Fisher Scientific) fluorescent secondary antibodies as well as DAPI. To determine the localization of the ER relative to the cytoskeleton, additional control cells were stained with rhodamine phalloidin (catalog no. R415, Thermo Fisher Scientific). Slides were then coverslipped with permafluor and visualized using the EVOS FL color imaging system at either ×20 or ×40 magnification.

Immunoblot Analysis—Cells were lysed in 4× SDS-PAGE sample buffer and separated on either 7 or 10% polyacrylamide gels in denaturing conditions, as described previously (84). Following gel electrophoresis, proteins were transferred to nitrocellulose membranes (Bio-Rad) using the Trans-Blot Semi-Dry transfer apparatus (Bio-Rad) and blocked with 5% skim milk (Compliments, Sobeys, Canada) in 1× TBS-T for 1 h at room temperature. Membranes were then incubated with primary antibodies for 18 h at 4 °C. The primary antibodies were diluted in 1× TBST with 1% skim milk. These included the following: anti-CHOP (catalog no. SC-793, Santa Cruz Biotechnology); anti-FLAG (catalog no. SC-121-G, Santa Cruz Biotechnology); anti-GRP78 (catalog no. 610979, BD Biosciences); anti-IRE1α (catalog no. 14C10 Cell Signaling Technology); anti-KDEL (catalog no. 10C3, Enzo Life Sciences); anti-PCSK9 (catalog no. NB300-959, Novus), and anti-SREBP2 (catalog no. 557037, BD Biosciences). Following the incubation with primary antibody, membranes were incubated with horseradish peroxidase-conjugated secondary antibodies diluted in 1× TBS-T with 1% milk (goat anti-mouse, catalog no. 170-6516, Bio-Rad; goat anti-rabbit, catalog no. 170-6515, Bio-Rad; and donkey anti-goat, catalog no. ab6741, Abcam). Membranes were visualized using the EZ-ECL chemiluminescent reagent (catalog no. 20-500-500, FroggaBio) on Amersham Biosciences Hyperfilm (catalog no. 28906839, GE Healthcare), which was subsequently developed on a Kodak X-Omat 1000A processor. Following exposure, band intensities were quantified using ImageJ software. Relative band intensities represent the mean of three replicate immunoblots adjusted to membranes re-probed against β-actin (catalog no. A5441, Sigma).

RT-PCR—Total RNA was isolated using RNeasy mini kits (catalog no. 74104, Qiagen) and reverse-transcribed to cDNA using SuperScript Vilo cDNA synthesis kit (catalog no. 11754050, Life Technologies, Inc.). RT-PCR was completed using Fast SYBR Green (catalog no.4385610, Life Technologies, Inc.), as described previously (83).

PCSK9 ELISA—Mouse plasma was diluted 1:200 and PCSK9 levels were determined using a mouse PCSK9 Quantikinine ELISA kit (catalog no.MCP900, R&D Systems). PCSK9 in tissue culture medium collected from cultured HuH7 cells grown in FBS-free medium was measured using the human PCSK9 quantikinine ELISA kit (catalog no. DCP900, R&D Systems).

Immunohistochemistry (IHC)—Liver tissues were collected and fixed in formaldehyde before being embedded in paraffin. Sections were subjected to antigen retrieval for 10 min at room temperature in 0.05% protease (Sigma) and stained for LDLR (catalog no. AF2255, R&D Systems), which was diluted 1:20. Quantification of LDLR staining was done using ImageJ software.

Animal Studies—Animal studies were separated into two independent experiments; the first aimed to identify the effect of ER stress on secreted PCSK9 levels, and the second was to examine the impact of ER stress on hepatic LDLR and circulating LDL levels. These experiments were completed using 12-week-old female C57BL/6 mice (strain no. 000664, Charles River, Sherbrooke, Quebec, Canada). Animals were received at 10 weeks of age and housed in 12:12 light/dark cycles and had access to rodent chow and water *ad libitum* for 2 weeks prior to studies. In our first experiment, which aimed to examine circulating PCSK9 and hepatic LDLR expression, animals were randomly divided into 8 groups ($n = 3$). Animals sacrificed 24 h following injection were treated with PBS vehicle control, TM 125 μg/kg, 250 μg/k, or 500 μg/kg (groups 1–4). The remaining animals were treated with TM 500 μg/kg and sacrificed every 24 h for 120 h. Plasma was collected via facial bleeds prior to the single subcutaneous injection and after sacrifice. In our second experiment, which aimed to examine circulating lipid, C57BL/6 mice were randomly divided into two groups ($n = 5$) and treated with either 1× PBS ($n = 5$) or TM 500 μg/kg ($n = 5$) for 24 h. In both experiments, liver tissue was flash-frozen for immunoblot and RT-PCR analyses or fixed in 4% formalin for IHC. The McMaster University Animal Research Ethics Board approved all procedures.

Plasma Lipoprotein Analysis—Total plasma cholesterol and triglycerides were determined using enzymatic kits (Wako Diagnostics, Richmond, VA). Plasma lipid profiles were generated via FPLC as described previously (85). In brief, 100 μl of plasma from each animal ($n = 3$) was fractioned by gel filtration FPLC using an AKTA system with a Tricorn Superose 6 HR10/300 column (GE Healthcare, Baie D'Urfe Quebec, Canada). An enzymatic assay kit was used to measure total cholesterol in fractionated plasma, following the manufacturer's instructions (catalog no. TR13421, Thermo Fisher Scientific, Ottawa, Ontario, Canada). Cholesterol from each fraction was quantified using a SpectraMax Plus384 spectrophotometer (Molecular Devices).

Statistical Analysis—Statistical analysis for differences between groups was performed using two-tailed unpaired

Student's *t* test. Comparisons between plasma PCSK9 concentrations from the same animals before and after treatment were completed using paired two-tailed Student's *t* test. Statistical tests were analyzed using Prism software (GraphPad Software, San Diego). Differences between groups were considered significant at $p < 0.05$, and all values are expressed as mean ± S.D.

Author Contributions—P. L., R. C. A., and N. G. S. conceived the studies. P. L. and S. S. performed all of the *in vitro* work, and P. L. and A. A. completed all of the *in vivo* studies. Immunohistochemical staining was completed by S. L., and fast protein liquid chromatography was performed by P. Y. and B. T. The manuscript was written by P. L. and revised by A. A., G. G., G. P., S. R. W. C., B. T., A. P., N. G. S., and R. C. A.

Acknowledgment—We thank Dr. Masayuki Miura (University of Tokyo) for the generous gift of the indicator plasmid used in this study.

References

1. Austin, R. C. (2009) The unfolded protein response in health and disease. *Antioxid. Redox Signal.* **11,** 2279–2287
2. Colgan, S. M., Hashimi, A. A., and Austin, R. C. (2011) Endoplasmic reticulum stress and lipid dysregulation. *Expert Rev. Mol. Med.* **13,** e4
3. Walter, P., and Ron, D. (2011) The unfolded protein response: from stress pathway to homeostatic regulation. *Science* **334,** 1081–1086
4. Corbett, E. F., Oikawa, K., Francois, P., Tessier, D. C., Kay, C., Bergeron, J. J., Thomas, D. Y., Krause, K. H., and Michalak, M. (1999) Ca^{2+} regulation of interactions between endoplasmic reticulum chaperones. *J. Biol. Chem.* **274,** 6203–6211
5. Tong, J., McCarthy, T. V., and MacLennan, D. H. (1999) Measurement of resting cytosolic Ca^{2+} concentrations and Ca^{2+} store size in HEK-293 cells transfected with malignant hyperthermia or central core disease mutant Ca^{2+} release channels. *J. Biol. Chem.* **274,** 693–702
6. Chen, W., Wang, R., Chen, B., Zhong, X., Kong, H., Bai, Y., Zhou, Q., Xie, C., Zhang, J., Guo, A., Tian, X., Jones, P. P., O'Mara, M. L., Liu, Y., Mi, T., *et al.* (2014) The ryanodine receptor store-sensing gate controls Ca^{2+} waves and Ca^{2+}-triggered arrhythmias. *Nat. Med.* **20,** 184–192
7. Lamb, H. K., Mee, C., Xu, W., Liu, L., Blond, S., Cooper, A., Charles, I. G., and Hawkins, A. R. (2006) The affinity of a major Ca^{2+}-binding site on GRP78 is differentially enhanced by ADP and ATP. *J. Biol. Chem.* **281,** 8796–8805
8. Biswas, C., Ostrovsky, O., Makarewich, C. A., Wanderling, S., Gidalevitz, T., and Argon, Y. (2007) The peptide-binding activity of GRP94 is regulated by calcium. *Biochem. J.* **405,** 233–241
9. Coe, H., and Michalak, M. (2009) Calcium binding chaperones of the endoplasmic reticulum. *Gen. Physiol. Biophys.* **28,** Spec. No. Focus, F96–F103
10. Corbett, E. F., and Michalak, M. (2000) Calcium, a signaling molecule in the endoplasmic reticulum? *Trends Biochem. Sci.* **25,** 307–311
11. Kaplowitz, N., Than, T. A., Shinohara, M., and Ji, C. (2007) Endoplasmic reticulum stress and liver injury. *Semin. Liver Dis.* **27,** 367–377
12. Dara, L., Ji, C., and Kaplowitz, N. (2011) The contribution of endoplasmic reticulum stress to liver diseases. *Hepatology* **53,** 1752–1763
13. Jo, H., Choe, S. S., Shin, K. C., Jang, H., Lee, J. H., Seong, J. K., Back, S. H., and Kim, J. B. (2013) Endoplasmic reticulum stress induces hepatic steatosis via increased expression of the hepatic very low density lipoprotein receptor. *Hepatology* **57,** 1366–1377
14. Lusis, A. J. (2000) Atherosclerosis. *Nature* **407,** 233–241
15. Tabas, I. (2010) Macrophage death and defective inflammation resolution in atherosclerosis. *Nat. Rev. Immunol.* **10,** 36–46
16. Pai, J. T., Brown, M. S., and Goldstein, J. L. (1996) Purification and cDNA cloning of a second apoptosis-related cysteine protease that cleaves and activates sterol regulatory element binding proteins. *Proc. Natl. Acad. Sci. U.S.A.* **93,** 5437–5442
17. Higgins, M. E., and Ioannou, Y. A. (2001) Apoptosis-induced release of mature sterol regulatory element-binding proteins activates sterol-responsive genes. *J. Lipid Res.* **42,** 1939–1946
18. Werstuck, G. H., Lentz, S. R., Dayal, S., Hossain, G. S., Sood, S. K., Shi, Y. Y., Zhou, J., Maeda, N., Krisans, S. K., Malinow, M. R., and Austin, R. C. (2001) Homocysteine-induced endoplasmic reticulum stress causes dysregulation of the cholesterol and triglyceride biosynthetic pathways. *J. Clin. Invest.* **107,** 1263–1273
19. Lee, J. N., and Ye, J. (2004) Proteolytic activation of sterol regulatory element-binding protein induced by cellular stress through depletion of Insig-1. *J. Biol. Chem.* **279,** 45257–45265
20. Colgan, S. M., Tang, D., Werstuck, G. H., and Austin, R. C. (2007) Endoplasmic reticulum stress causes the activation of sterol regulatory element binding protein-2. *Int. J. Biochem. Cell Biol.* **39,** 1843–1851
21. Lauressergues, E., Bert, E., Duriez, P., Hum, D., Majd, Z., Staels, B., and Cussac, D. (2012) Does endoplasmic reticulum stress participate in APD-induced hepatic metabolic dysregulation? *Neuropharmacology* **62,** 784–796
22. Lhoták, S., Sood, S., Brimble, E., Carlisle, R. E., Colgan, S. M., Mazzetti, A., Dickhout, J. G., Ingram, A. J., and Austin, R. C. (2012) ER stress contributes to renal proximal tubule injury by increasing SREBP-2-mediated lipid accumulation and apoptotic cell death. *Am. J. Physiol. Renal Physiol.* **303,** F266–F278
23. Vig, S., Talwar, P., Kaur, K., Srivastava, R., Srivastava, A. K., and Datta, M. (2015) Transcriptome profiling identifies p53 as a key player during calreticulin deficiency: Implications in lipid accumulation. *Cell Cycle* **14,** 2274–2284
24. Hua, X., Nohturfft, A., Goldstein, J. L., and Brown, M. S. (1996) Sterol resistance in CHO cells traced to point mutation in SREBP cleavage-activating protein. *Cell* **87,** 415–426
25. Yabe, D., Brown, M. S., and Goldstein, J. L. (2002) Insig-2, a second endoplasmic reticulum protein that binds SCAP and blocks export of sterol regulatory element-binding proteins. *Proc. Natl. Acad. Sci. U.S.A.* **99,** 12753–12758
26. Sun, L. P., Li, L., Goldstein, J. L., and Brown, M. S. (2005) Insig required for sterol-mediated inhibition of Scap/SREBP binding to COPII proteins *in vitro*. *J. Biol. Chem.* **280,** 26483–26490
27. Sakai, J., Duncan, E. A., Rawson, R. B., Hua, X., Brown, M. S., and Goldstein, J. L. (1996) Sterol-regulated release of SREBP-2 from cell membranes requires two sequential cleavages, one within a transmembrane segment. *Cell* **85,** 1037–1046
28. Nohturfft, A., Brown, M. S., and Goldstein, J. L. (1998) Sterols regulate processing of carbohydrate chains of wild-type SREBP cleavage-activating protein (SCAP), but not sterol-resistant mutants Y298C or D443N. *Proc. Natl. Acad. Sci. U.S.A.* **95,** 12848–12853
29. Nohturfft, A., DeBose-Boyd, R. A., Scheek, S., Goldstein, J. L., and Brown, M. S. (1999) Sterols regulate cycling of SREBP cleavage-activating protein (SCAP) between endoplasmic reticulum and Golgi. *Proc. Natl. Acad. Sci. U.S.A.* **96,** 11235–11240
30. Goldstein, J. L., DeBose-Boyd, R. A., and Brown, M. S. (2006) Protein sensors for membrane sterols. *Cell* **124,** 35–46
31. Horton, J. D., Shah, N. A., Warrington, J. A., Anderson, N. N., Park, S. W., Brown, M. S., and Goldstein, J. L. (2003) Combined analysis of oligonucleotide microarray data from transgenic and knockout mice identifies direct SREBP target genes. *Proc. Natl. Acad. Sci. U.S.A.* **100,** 12027–12032
32. Seidah, N. G., Benjannet, S., Wickham, L., Marcinkiewicz, J., Jasmin, S. B., Stifani, S., Basak, A., Prat, A., and Chretien, M. (2003) The secretory proprotein convertase neural apoptosis-regulated convertase 1 (NARC-1): liver regeneration and neuronal differentiation. *Proc. Natl. Acad. Sci. U.S.A.* **100,** 928–933
33. Abifadel, M., Varret, M., Rabès, J. P., Allard, D., Ouguerram, K., Devillers, M., Cruaud, C., Benjannet, S., Wickham, L., Erlich, D., Derré, A., Villéger, L., Farnier, M., Beucler, I., Bruckert, E., *et al.* (2003) Mutations in PCSK9 cause autosomal dominant hypercholesterolemia. *Nat. Genet.* **34,** 154–156
34. Benjannet, S., Rhainds, D., Essalmani, R., Mayne, J., Wickham, L., Jin, W., Asselin, M. C., Hamelin, J., Varret, M., Allard, D., Trillard, M., Abifadel, M., Tebon, A., Attie, A. D., Rader, D. J., *et al.* (2004) NARC-1/PCSK9

and its natural mutants: zymogen cleavage and effects on the low density lipoprotein (LDL) receptor and LDL cholesterol. *J. Biol. Chem.* **279,** 48865–48875
35. Lagace, T. A., Curtis, D. E., Garuti, R., McNutt, M. C., Park, S. W., Prather, H. B., Anderson, N. N., Ho, Y. K., Hammer, R. E., and Horton, J. D. (2006) Secreted PCSK9 decreases the number of LDL receptors in hepatocytes and in livers of parabiotic mice. *J. Clin. Invest.* **116,** 2995–3005
36. Zhang, D. W., Lagace, T. A., Garuti, R., Zhao, Z., McDonald, M., Horton, J. D., Cohen, J. C., and Hobbs, H. H. (2007) Binding of proprotein convertase subtilisin/kexin type 9 to epidermal growth factor-like repeat A of low density lipoprotein receptor decreases receptor recycling and increases degradation. *J. Biol. Chem.* **282,** 18602–18612
37. Maxwell, K. N., and Breslow, J. L. (2004) Adenoviral-mediated expression of Pcsk9 in mice results in a low density lipoprotein receptor knockout phenotype. *Proc. Natl. Acad. Sci. U.S.A.* **101,** 7100–7105
38. Inui, M., Saito, A., and Fleischer, S. (1987) Purification of the ryanodine receptor and identity with feet structures of junctional terminal cisternae of sarcoplasmic reticulum from fast skeletal muscle. *J. Biol. Chem.* **262,** 1740–1747
39. Inui, M., and Fleischer, S. (1988) Purification of Ca^{2+} release channel (ryanodine receptor) from heart and skeletal muscle sarcoplasmic reticulum. *Methods Enzymol.* **157,** 490–505
40. Lai, F. A., Erickson, H. P., Rousseau, E., Liu, Q. Y., and Meissner, G. (1988) Purification and reconstitution of the calcium release channel from skeletal muscle. *Nature* **331,** 315–319
41. Chen, Y. F., Chiu, W. T., Chen, Y. T., Lin, P. Y., Huang, H. J., Chou, C. Y., Chang, H. C., Tang, M. J., and Shen, M. R. (2011) Calcium store sensor stromal-interaction molecule 1-dependent signaling plays an important role in cervical cancer growth, migration, and angiogenesis. *Proc. Natl. Acad. Sci. U.S.A.* **108,** 15225–15230
42. Jones, P. P., Jiang, D., Bolstad, J., Hunt, D. J., Zhang, L., Demaurex, N., and Chen, S. R. (2008) Endoplasmic reticulum Ca^{2+} measurements reveal that the cardiac ryanodine receptor mutations linked to cardiac arrhythmia and sudden death alter the threshold for store-overload-induced Ca^{2+} release. *Biochem. J.* **412,** 171–178
43. Cenedella, R. J. (2009) Cholesterol synthesis inhibitor U18666A and the role of sterol metabolism and trafficking in numerous pathophysiological processes. *Lipids* **44,** 477–487
44. Schuck, S., Prinz, W. A., Thorn, K. S., Voss, C., and Walter, P. (2009) Membrane expansion alleviates endoplasmic reticulum stress independently of the unfolded protein response. *J. Cell Biol.* **187,** 525–536
45. Benjannet, S., Hamelin, J., Chrétien, M., and Seidah, N. G. (2012) Loss- and gain-of-function PCSK9 variants: cleavage specificity, dominant negative effects, and low density lipoprotein receptor (LDLR) degradation. *J. Biol. Chem.* **287,** 33745–33755
46. Zaid, A., Roubtsova, A., Essalmani, R., Marcinkiewicz, J., Chamberland, A., Hamelin, J., Tremblay, M., Jacques, H., Jin, W., Davignon, J., Seidah, N. G., and Prat, A. (2008) Proprotein convertase subtilisin/kexin type 9 (PCSK9): hepatocyte-specific low density lipoprotein receptor degradation and critical role in mouse liver regeneration. *Hepatology* **48,** 646–654
47. Greeve, J., Altkemper, I., Dieterich, J. H., Greten, H., and Windler, E. (1993) Apolipoprotein B mRNA editing in 12 different mammalian species: hepatic expression is reflected in low concentrations of apoB-containing plasma lipoproteins. *J. Lipid Res.* **34,** 1367–1383
48. Song, Y. F., Luo, Z., Zhang, L. H., Hogstrand, C., and Pan, Y. X. (2016) Endoplasmic reticulum stress and disturbed calcium homeostasis are involved in copper-induced alteration in hepatic lipid metabolism in yellow catfish *Pelteobagrus fulvidraco*. *Chemosphere* **144,** 2443–2453
49. Poirier, S., Mamarbachi, M., Chen, W. T., Lee, A. S., and Mayer, G. (2015) GRP94 regulates circulating cholesterol levels through blockade of PCSK9-induced LDLR degradation. *Cell Rep.* **13,** 2064–2071
50. Chen, X. W., Wang, H., Bajaj, K., Zhang, P., Meng, Z. X., Ma, D., Bai, Y., Liu, H. H., Adams, E., Baines, A., Yu, G., Sartor, M. A., Zhang, B., Yi, Z., Lin, J., *et al.* (2013) SEC24A deficiency lowers plasma cholesterol through reduced PCSK9 secretion. *eLife* **2,** e00444
51. Amodio, G., Venditti, R., De Matteis, M. A., Moltedo, O., Pignataro, P., and Remondelli, P. (2013) Endoplasmic reticulum stress reduces COPII vesicle formation and modifies Sec23a cycling at ERESs. *FEBS Lett.* **587,** 3261–3266
52. Roubtsova, A., Chamberland, A., Marcinkiewicz, J., Essalmani, R., Fazel, A., Bergeron, J. J., Seidah, N. G., and Prat, A. (2015) PCSK9 deficiency unmasks a sex- and tissue-specific subcellular distribution of the LDL and VLDL receptors in mice. *J. Lipid Res.* **56,** 2133–2142
53. Basseri, S., Lhoták, S., Sharma, A. M., and Austin, R. C. (2009) The chemical chaperone 4-phenylbutyrate inhibits adipogenesis by modulating the unfolded protein response. *J. Lipid Res.* **50,** 2486–2501
54. Park, S. W., Moon, Y. A., and Horton, J. D. (2004) Post-transcriptional regulation of low density lipoprotein receptor protein by proprotein convertase subtilisin/kexin type 9a in mouse liver. *J. Biol. Chem.* **279,** 50630–50638
55. Grefhorst, A., McNutt, M. C., Lagace, T. A., and Horton, J. D. (2008) Plasma PCSK9 preferentially reduces liver LDL receptors in mice. *J. Lipid Res.* **49,** 1303–1311
56. Strøm, T. B., Tveten, K., and Leren, T. P. (2014) PCSK9 acts as a chaperone for the LDL receptor in the endoplasmic reticulum. *Biochem. J.* **457,** 99–105
57. Horton, J. D., Goldstein, J. L., and Brown, M. S. (2002) SREBPs: activators of the complete program of cholesterol and fatty acid synthesis in the liver. *J. Clin. Invest.* **109,** 1125–1131
58. Cheng, C., Ru, P., Geng, F., Liu, J., Yoo, J. Y., Wu, X., Cheng, X., Euthine, V., Hu, P., Guo, J. Y., Lefai, E., Kaur, B., Nohturfft, A., Ma, J., Chakravarti, A., and Guo, D. (2015) Glucose-mediated *N*-glycosylation of SCAP is essential for SREBP-1 activation and tumor growth. *Cancer Cell* **28,** 569–581
59. Volpe, J. J., and Goldberg, R. I. (1983) Effect of tunicamycin on 3-hydroxy-3-methylglutaryl coenzyme A reductase in C-6 glial cells. *J. Biol. Chem.* **258,** 9220–9226
60. Röhrl, C., Eigner, K., Winter, K., Korbelius, M., Obrowsky, S., Kratky, D., Kovacs, W. J., and Stangl, H. (2014) Endoplasmic reticulum stress impairs cholesterol efflux and synthesis in hepatic cells. *J. Lipid Res.* **55,** 94–103
61. Choi, S., Aljakna, A., Srivastava, U., Peterson, B. R., Deng, B., Prat, A., and Korstanje, R. (2013) Decreased APOE-containing HDL subfractions and cholesterol efflux capacity of serum in mice lacking Pcsk9. *Lipids Health Dis.* **12,** 112
62. Tran, H., Robinson, S., Mikhailenko, I., and Strickland, D. K. (2003) Modulation of the LDL receptor and LRP levels by HIV protease inhibitors. *J. Lipid Res.* **44,** 1859–1869
63. Holtzman, D. M., Herz, J., and Bu, G. (2012) Apolipoprotein E and apolipoprotein E receptors: normal biology and roles in Alzheimer disease. *Cold Spring Harb. Perspect. Med.* **2,** a006312
64. Rashid, S., Curtis, D. E., Garuti, R., Anderson, N. N., Bashmakov, Y., Ho, Y. K., Hammer, R. E., Moon, Y. A., and Horton, J. D. (2005) Decreased plasma cholesterol and hypersensitivity to statins in mice lacking Pcsk9. *Proc. Natl. Acad. Sci. U.S.A.* **102,** 5374–5379
65. Poirier, S., Mayer, G., Benjannet, S., Bergeron, E., Marcinkiewicz, J., Nassoury, N., Mayer, H., Nimpf, J., Prat, A., and Seidah, N. G. (2008) The proprotein convertase PCSK9 induces the degradation of low density lipoprotein receptor (LDLR) and its closest family members VLDLR and ApoER2. *J. Biol. Chem.* **283,** 2363–2372
66. Roubtsova, A., Munkonda, M. N., Awan, Z., Marcinkiewicz, J., Chamberland, A., Lazure, C., Cianflone, K., Seidah, N. G., and Prat, A. (2011) Circulating proprotein convertase subtilisin/kexin 9 (PCSK9) regulates VLDLR protein and triglyceride accumulation in visceral adipose tissue. *Arterioscler. Thromb. Vasc. Biol.* **31,** 785–791
67. Canuel, M., Sun, X., Asselin, M. C., Paramithiotis, E., Prat, A., and Seidah, N. G. (2013) Proprotein convertase subtilisin/kexin type 9 (PCSK9) can mediate degradation of the low density lipoprotein receptor-related protein 1 (LRP-1). *PLoS ONE* **8,** e64145
68. Jin, W., Wang, X., Millar, J. S., Quertermous, T., Rothblat, G. H., Glick, J. M., and Rader, D. J. (2007) Hepatic proprotein convertases modulate HDL metabolism. *Cell Metab.* **6,** 129–136
69. Chorba, J. S., and Shokat, K. M. (2014) The proprotein convertase subtilisin/kexin type 9 (PCSK9) active site and cleavage sequence differentially regulate protein secretion from proteolysis. *J. Biol. Chem.* **289,** 29030–29043

70. Gustafsen, C., Kjolby, M., Nyegaard, M., Mattheisen, M., Lundhede, J., Buttenschøn, H., Mors, O., Bentzon, J. F., Madsen, P., Nykjaer, A., and Glerup, S. (2014) The hypercholesterolemia-risk gene SORT1 facilitates PCSK9 secretion. *Cell Metab.* **19,** 310–318
71. Butkinaree, C., Canuel, M., Essalmani, R., Poirier, S., Benjannet, S., Asselin, M. C., Roubtsova, A., Hamelin, J., Marcinkiewicz, J., Chamberland, A., Guillemot, J., Mayer, G., Sisodia, S. S., Jacob, Y., Prat, A., and Seidah, N. G. (2015) Amyloid precursor-like protein 2 and sortilin do not regulate the PCSK9 convertase-mediated low density lipoprotein receptor degradation but interact with each other. *J. Biol. Chem.* **290,** 18609–18620
72. Seidah, N. G. (2015) The PCSK9 revolution and the potential of PCSK9-based therapies to reduce LDL-cholesterol. *Global Cardiology Science and Practice* **59,** 1–19
73. McNutt, M. C., Kwon, H. J., Chen, C., Chen, J. R., Horton, J. D., and Lagace, T. A. (2009) Antagonism of secreted PCSK9 increases low density lipoprotein receptor expression in HepG2 cells. *J. Biol. Chem.* **284,** 10561–10570
74. Kosenko, T., Golder, M., Leblond, G., Weng, W., and Lagace, T. A. (2013) Low density lipoprotein binds to proprotein convertase subtilisin/kexin type-9 (PCSK9) in human plasma and inhibits PCSK9-mediated low density lipoprotein receptor degradation. *J. Biol. Chem.* **288,** 8279–8288
75. Jiang, D., Wang, R., Xiao, B., Kong, H., Hunt, D. J., Choi, P., Zhang, L., and Chen, S. R. (2005) Enhanced store overload-induced Ca^{2+} release and channel sensitivity to luminal Ca^{2+} activation are common defects of RyR2 mutations linked to ventricular tachycardia and sudden death. *Circ. Res.* **97,** 1173–1181
76. Jiang, D., Jones, P. P., Davis, D. R., Gow, R., Green, M. S., Birnie, D. H., Chen, S. R., and Gollob, M. H. (2010) Characterization of a novel mutation in the cardiac ryanodine receptor that results in catecholaminergic polymorphic ventricular tachycardia. *Channels* **4,** 302–310
77. Merlie, J. P., Sebbane, R., Tzartos, S., and Lindstrom, J. (1982) Inhibition of glycosylation with tunicamycin blocks assembly of newly synthesized acetylcholine receptor subunits in muscle cells. *J. Biol. Chem.* **257,** 2694–2701
78. Kamisuki, S., Mao, Q., Abu-Elheiga, L., Gu, Z., Kugimiya, A., Kwon, Y., Shinohara, T., Kawazoe, Y., Sato, S., Asakura, K., Choo, H. Y., Sakai, J., Wakil, S. J., and Uesugi, M. (2009) A small molecule that blocks fat synthesis by inhibiting the activation of SREBP. *Chem. Biol.* **16,** 882–892
79. Hawkins, J. L., Robbins, M. D., Warren, L. C., Xia, D., Petras, S. F., Valentine, J. J., Varghese, A. H., Wang, I. K., Subashi, T. A., Shelly, L. D., Hay, B. A., Landschulz, K. T., Geoghegan, K. F., and Harwood, H. J., Jr. (2008) Pharmacologic inhibition of site 1 protease activity inhibits sterol regulatory element-binding protein processing and reduces lipogenic enzyme gene expression and lipid synthesis in cultured cells and experimental animals. *J. Pharmacol. Exp. Ther.* **326,** 801–808
80. Fullerton, M. D., Galic, S., Marcinko, K., Sikkema, S., Pulinilkunnil, T., Chen, Z. P., O'Neill, H. M., Ford, R. J., Palanivel, R., O'Brien, M., Hardie, D. G., Macaulay, S. L., Schertzer, J. D., Dyck, J. R., van Denderen, B. J., *et al.* (2013) Single phosphorylation sites in Acc1 and Acc2 regulate lipid homeostasis and the insulin-sensitizing effects of metformin. *Nat. Med.* **19,** 1649–1654
81. Gonzalez-Gronow, M., Gawdi, G., and Pizzo, S. V. (1993) Plasminogen activation stimulates an increase in intracellular calcium in human synovial fibroblasts. *J. Biol. Chem.* **268,** 20791–20795
82. Iwawaki, T., Akai, R., Kohno, K., and Miura, M. (2004) A transgenic mouse model for monitoring endoplasmic reticulum stress. *Nat. Med.* **10,** 98–102
83. Mayne, J., Dewpura, T., Raymond, A., Bernier, L., Cousins, M., Ooi, T. C., Davignon, J., Seidah, N. G., Mbikay, M., and Chrétien, M. (2011) Novel loss-of-function PCSK9 variant is associated with low plasma LDL cholesterol in a French-Canadian family and with impaired processing and secretion in cell culture. *Clin. Chem.* **57,** 1415–1423
84. Al-Hashimi, A. A., Caldwell, J., Gonzalez-Gronow, M., Pizzo, S. V., Aboumrad, D., Pozza, L., Al-Bayati, H., Weitz, J. I., Stafford, A., Chan, H., Kapoor, A., Jacobsen, D. W., Dickhout, J. G., and Austin, R. C. (2010) Binding of anti-GRP78 autoantibodies to cell surface GRP78 increases tissue factor procoagulant activity via the release of calcium from endoplasmic reticulum stores. *J. Biol. Chem.* **285,** 28912–28923
85. Fuller, M., Dadoo, O., Serkis, V., Abutouk, D., MacDonald, M., Dhingani, N., Macri, J., Igdoura, S. A., and Trigatti, B. L. (2014) The effects of diet on occlusive coronary artery atherosclerosis and myocardial infarction in scavenger receptor class B, type 1/low density lipoprotein receptor double knockout mice. *Arterioscler. Thromb. Vasc. Biol.* **34,** 2394–2403